EAST EUROPEAN JOURNAL OF PHYSICS. 1. 308-317 (2026)
DOI:10.26565/2312-4334-2026-1-36 ISSN 2312-4334

FIRST-PRINCIPLES INVESTIGATION OF ELECTRONIC AND MAGNETIC PROPERTIES IN Ga-DOPED SILICON CARBIDE NANOTUBES

Vusala Nabi Jafarova[1]*, Khayala Ajdar Hasanova[1,2], Adile Adem Guliyeva[3], Vusala Irshad Eminova[4], Ionut Cristian Scurtu[5]

[1]*Azerbaijan State Oil and Industry University, 20 Azalig Ave., AZ-1010, Baku, Azerbaijan*
[2]*Ministry of Science and Education Republic of Azerbaijan, Institute of Physics, 131 H. Javid Ave., AZ-1143, Baku, Azerbaijan*
[3]*Nakhchivan State University, AZ-7012, Nakhchivan, Azerbaijan*
[4]*French-Azerbaijani University (UFAZ) under Azerbaijan State Oil and Industry University, 183 Nizami Street, AZ-1010, Baku, Azerbaijan*
[5]*Mircea cel Batran Naval Academy, Str. Fulgerului, nr.1, 900218 Constanța, Romania*
**Corresponding Author E-mail: vusala.cafarova@asoiu.edu.az*
Received September 27, 2025; revised January 30, 2026; accepted February 2, 2026

This work explores the electronic and magnetic characteristics of gallium (Ga)-doped silicon carbide nanotubes (SiCNTs) through first-principles calculations. Two doping levels (8.3% and 16.6%) are considered, with Ga atoms substituting silicon sites in single-walled (6,0) SiCNTs. Spin-polarized band structure analysis shows that the system transitions from semiconducting at low doping to half-metallic at high doping, suggesting strong potential for spintronic applications. Density of states and Bader charge analyses reveal that Ga incorporation alters charge distribution and orbital interactions, particularly between Ga 5d and carbon 2p states. Magnetic moment calculations indicate that Ga induces localized magnetism primarily on neighboring carbon atoms, with the overall net magnetization increasing with increasing doping level. Energy comparisons between ferromagnetic and antiferromagnetic configurations point to an antiferromagnetic ground state, while formation energy evaluations confirm that Ga substitution at Si sites is thermodynamically favorable. Collectively, these results underscore Ga-doped SiCNTs as promising, tunable materials for future nanoscale electronic and spintronic devices.
Keywords: *SiC:Ga; Nanotube; Magnetic moment; Half-metallic*
PACS: 61.43.Bn; 71.20.-b; 73.22. -f; 75.50. Gg; 75.50. Pp; 78.67. Ch

1. INTRODUCTION

Graphene-like and other two-dimensional (2D) semiconductor materials have recently attracted increasing research attention because their unique physical and chemical properties enable promising applications in spintronic and optoelectronic devices, as demonstrated in recent reviews of emerging 2D materials with prospects in electronics, optoelectronics, and spintronics [1-3]. Silicon carbide (SiC), a third-generation wide-bandgap semiconductor, has become indispensable in high-voltage, high-temperature, high-frequency, and high-power devices due to its large band gap, high breakdown field, excellent thermal conductivity, chemical stability, and mechanical robustness, as demonstrated in studies on its superior performance in power electronics and thermal management furthermore, beyond traditional electronic applications, SiC has been recognized as a biocompatible and hemocompatible material suitable for advanced biomedical applications, including implantable devices, biosensing, and tissue engineering and more recently, its unique physical and electronic characteristics have enabled innovative roles in energy harvesting systems such as photovoltage generation and piezoelectric harvesting for harsh-environment applications [1-9].

Both theoretical and experimental studies have shown that silicon carbide nanotubes (SiCNTs) exhibit more stable electronic and magnetic properties than carbon nanotubes (CNTs) [2-6]. To broaden the applications of 1D, 2D, and 3D Si-based nanomaterials, researchers have increasingly explored doping with different impurity atoms to fine-tune their physical properties. Metal- and transition-metal-doped single-walled SiCNTs (SWSiCNTs) have demonstrated strong potential for applications in chemical sensing, hydrogen storage, and nanoscale spintronic devices. The incorporation of dopants alters charge distribution within the nanotube framework and can induce magnetic behavior. In most cases, the observed ferromagnetic (FM) characteristics originate from the hybridization between the dopants' d orbitals and the surrounding SiCNT states [10, 11].

Previous density functional theory (DFT) studies have confirmed that the electronic and magnetic properties of SiCNTs can be effectively tuned through doping. For example, Fe-doped SiCNTs were reported to exhibit either half-metallic antiferromagnetic (AFM) or ferromagnetic (FM) states depending on the substitution site of the dopant [1]. The adsorption of various transition metals (TMs) on SWSiCNTs was also investigated, revealing strong chemical binding with adsorption energies ranging from 1.17 eV (Cu) to 3.18 eV (Pt) [12]. Co doping has been shown to induce metallic behavior in cubic SiC, while Mn- and Fe-doped (8,0) SiCNTs displayed half-metallicity, making them promising for spintronic applications [13,14]. Furthermore, studies of the electronic and optical properties of different SiCNT chiralities have consistently confirmed their indirect-bandgap semiconducting nature [15,16].

Cite as: V.N. Jafarova, K.A. Hasanova, A.A. Guliyeva, V.I. Eminova, I.C. Scurtu, East Eur. J. Phys. 1, 308 (2026), https://doi.org/10.26565/2312-4334-2026-1-36

Silicon and carbon, due to their similar valence electron configurations, have long been predicted to form fullerene-like and nanotube structures, including chiral (6,0) SWSiCNTs [17]. Recent first-principles studies, including those that incorporate machine learning into DFT, have shown that noble-metal doping (e.g., Ag and Au) can endow SiCNTs with tunable magnetic properties suitable for spintronic applications [18–20]. These computational approaches also allow accurate predictions of electronic density of states and magnetic transitions under different doping conditions [21]. In particular, transition-metal dopants such as V and Co have been found to induce strong ferromagnetism and high Curie temperatures in SiCNTs, further supporting their potential in magnetic devices [20, 22, 23].

Beyond transition metals, group-III element doping has recently attracted interest. Studies on Al- and P-doped (6,0) SiCNTs revealed that Al substitution can significantly modulate electronic properties, suggesting controllable semiconducting behavior [24]. Related investigations on Al- and Ga-doped boron nitride nanotubes demonstrated enhanced CO adsorption energies [25] and improved surface reactivity toward H_2SiCl_2 [26], indicating that group-III elements enhance chemical sensitivity and surface interactions. Further DFT work on Al-doped carbon nanotubes confirmed improved adsorption of sulfur-containing gases, emphasizing the functional role of p-block dopants in tuning nanotube properties [27].

The motivation for this research is to identify new spintronic materials with tunable magnetic properties. Doping SiCNTs with group-III elements such as Ga offers a promising pathway, as these dopants introduce unique electronic and magnetic modifications distinct from transition metals. Unlike metallic dopants, p-block elements can yield stable, lightweight, and non-toxic spintronic materials. Investigating Al- and Ga-doped SWSiCNT systems therefore provides insight into how such dopants influences spin polarization and magnetic moment distribution, potentially enabling the design of non-magnetic-element-based spintronic nanodevices.

In addition to spintronics, doped nanotubes can stabilize isolated atoms, serving as active sites for single-atom catalysis (SAC). While SAC studies on Ga-doped SiCNTs are limited, similar behavior in doped graphene and other 2D systems suggests that Ga substitution may also enhance catalytic activity in SiCNTs [28]. Moreover, due to their chemical stability, high surface area, and tunable surface reactivity, doped SiC nanostructures are widely investigated for energy-related applications, including hydrogen storage, photocatalysis, and electrode materials for energy conversion and storage [29, 30]. Adharsh et al. [31] demonstrated that surface functionalization of (5,5) SiC nanotubes can form thermodynamically stable configurations with negative binding energies and significantly modify the electronic structure by tuning the band gap, confirming the high sensitivity of SiCNT electronic properties to chemical/atomic-level modifications. This supports the motivation of our work, where Ga doping is employed as an alternative and effective route to tailor the electronic and magnetic response of SiC nanotubes via first-principles calculations. Vlaskina et al. [32] investigated defect-related photoluminescence in SiC crystals and showed that stacking faults and deep-level defects introduce characteristic electronic states that strongly depend on the SiC polytype structure. Their findings highlight that imperfections and foreign-atom–induced states can critically reshape the electronic spectrum of SiC-based systems, which is directly relevant to our first-principles investigation of how Ga doping modifies the electronic and magnetic properties of SiC nanotubes.

2. COMPUTATIONAL DETAILS

In this study, first-principles calculations were carried out using the Atomistix ToolKit (ATK V-2023.09, http://quantumwise.com/) simulation package to examine the electronic and magnetic properties of Ga-doped SWSiCNTs. The modeled systems consisted of 24 atoms per unit cell. All calculations were performed within the framework of density functional theory (DFT) [31], employing the Local Spin Density Approximation (LSDA) [32] for the exchange-correlation potential, with FHI-type pseudopotentials [33] used to describe electron-ion interactions.

DFT is a quantum-mechanical modeling approach for investigating the electronic structure of many-body systems such as atoms, molecules, and solids. Rather than solving the full many-body Schrödinger equation, DFT reformulates the problem in terms of the electron density, ρ(r), as the primary variable. The central framework is based on the Kohn–Sham equations, which are obtained by minimizing the total energy functional with respect to the electron density. To account for magnetic effects, spin-polarized DFT was employed. Within this framework, LSDA serves as a reliable method for describing systems with unpaired electrons, localized magnetic moments, and magnetic ordering. In LSDA, the total electron density is divided into spin-up (ρ↑) and spin-down (ρ↓) components, allowing the evaluation of spin-dependent interactions. The total spin magnetization (M) of the system is defined as:

$$M = \int [\rho^{\uparrow}(r) - \rho^{\downarrow}(r)] dr \,. \tag{1}$$

It is well established that standard DFT implementations often underestimate semiconductor band gaps. To overcome this limitation, the DFT+U method, specifically the Local Spin Density Approximation with Hubbard U (LSDA+U) [34], introduces an on-site Coulomb interaction term to better describe localized electrons. Semi-empirical Hubbard U values were employed to enhance the accuracy of the electronic structure: a U_d of 5 eV was applied to the Si d-orbitals, while a U_p of 4.8 eV was assigned to the C p-orbitals, ensuring more reliable reproduction of the system's band gap. This correction is crucial in cases where LSDA suffers from self-interaction errors. Incorporating semi-empirical Hubbard U corrections [34] has significantly improved the predictive accuracy of semiconductor band gaps. In this work, the Hubbard U parameter was applied following simplified schemes reported in Refs. [35, 36].

In the spin-polarized DFT framework, both the Hamiltonian and density matrices were extended to include spin degrees of freedom, thereby allowing independent treatment of spin-up and spin-down channels. This formalism enables a more accurate description of magnetic properties and spin asymmetry in the electronic structure. Calculations were performed under the collinear spin approximation, which assumes all magnetic moments are aligned either parallel or antiparallel. This is a reasonable assumption for systems dominated by localized 3d transition-metal dopants in SiC nanotubes, where non-collinear magnetic effects are negligible.

The LSDA functional was chosen due to its computational efficiency and proven effectiveness in capturing spin polarization in transition-metal-doped semiconductors. Spin-resolved density of states (DOS) and magnetic moments were analyzed using Mulliken population analysis [37], which provides detailed insight into the spatial origin and distribution of magnetization. The spin density distribution, defined as $\rho\uparrow - \rho\downarrow$, was further examined to evaluate spin localization and magnetic interactions near the dopant sites.

Mulliken population analysis [37], a classical method in quantum chemistry, was employed to compute the local magnetic moments of 3d transition-metal-doped SWSiCNTs. By partitioning the electron density among atoms and orbitals, this approach allows estimation of atomic charges, orbital contributions, and bond populations. Within spin-polarized DFT, the electron density is divided into α-spin (spin-up) and β-spin (spin-down) components. The local spin magnetic moment on an atom A is defined as the difference between its α- and β-spin Mulliken populations:

$$\mu^A = N_\alpha^A - N_\beta^A \tag{2}$$

where N_α^A and N_β^A represent the numbers of spin-up and spin-down electrons assigned to atom A, respectively.

A nonzero value of μ^A indicates the presence of a local magnetic moment. The sign and magnitude of μ^A provide valuable information on the nature of magnetic ordering and spin coupling within the system. This formalism enabled us to quantify the magnetic contributions of dopant atoms as well as neighboring Si and C atoms in the nanotube framework. For doped SWSiCNTs, the partially filled 3d orbitals of transition-metal dopants typically introduce localized unpaired electrons, which lead to significant magnetic moments. Mulliken population analysis was employed not only to determine the magnitude of these local moments but also to reveal their spatial distribution between the Ga dopant and nearby Si and C atoms in the nanotube lattice. This information is essential for understanding the origin of magnetism in doped SiCNTs and their potential applications in spintronic or magnetic-sensing devices. Mulliken population analysis was also used to obtain orbital occupation numbers, from which magnetic moments were calculated as the difference between spin-up and spin-down populations. Partial density of states (PDOS) for each spin channel was determined using a Lorentzian broadening function [38], which smooths the discrete one-electron eigenvalues for graphical representation. The broadened PDOS is expressed as:

$$D_{nl\sigma}^{\alpha}(E) = \sum_i A_{nl\sigma i}^{\alpha} \frac{\delta/\pi}{\left(E - \varepsilon_{i\sigma}\right)^2 + \delta^2}, \tag{3}$$

let $\varepsilon_{i\sigma}$ denote the one-electron energies, where i is index of the energy level, and σ represents the spin state. The function $A_{nl\sigma i}^{\alpha}$ refers to the atomic orbital localized on atom α.

The total density of states (TDOS) is obtained by summing the projected density of states (PDOS) contributions for atom α at a given energy E. This requires a summation over all orbitals of atom α, characterized by the quantum numbers (n,l), as well as over both spin states (σ). The expression is typically written as Eq. (4):

$$D_\sigma(E) = \sum_{nl\alpha} D_{nl\sigma}^{\alpha}(E). \tag{4}$$

The quantum-confined SWSiCNT with a chiral vector of (6,0) was theoretically modeled using DFT method. To explore its electronic and magnetic behavior, Ga atoms were introduced as substitutional dopants. For Brillouin zone sampling, a Monkhorst-Pack grid of 1×1×5 k-points [39] was used, providing dense coverage along the nanotube's periodic z-axis. The plane-wave cutoff energy was set to 50 Ha, and all geometries were fully optimized at an electron temperature of 300 K. Convergence thresholds were chosen as <0.001 eV/Å for atomic forces and <0.001 eV/Å³ for cell stress. The valence electron configurations considered were: silicon ($3s^2 3p^2$, 4 valence electrons), carbon ($2s^2 2p^2$, 4 valence electrons), and gallium ($4s^2 4p^1$, 3 valence electrons).

This study specifically addresses the influence of Ga doping concentration on the structural, electronic, and magnetic properties of SiCNTs. Two substitutional cases were considered: Ga replacing Si atoms and Ga replacing C atoms. Single doping corresponds to a concentration of 8.3%, while double doping corresponds to 16.6%. By comparing these doping schemes, the impact of dopant type, substitutional site, and concentration on the system's fundamental properties was systematically investigated. Such insights are essential for tailoring SiCNTs for potential nanoelectronic and spintronic applications.

To further examine magnetic ordering, both ferromagnetic (FM) and antiferromagnetic (AFM) configurations were modeled by substituting Si atoms with Ga. In the FM case, dopants carried parallel spins (Ga ↑ x/2; Ga ↑ x/2),

whereas in the AFM case, the spins were antiparallel (Ga ↑ x/2; Ga ↓ x/2). Here, ↑ and ↓ indicate the orientation of the local magnetic moments associated with the Ga dopants.

RESULTS AND DISCUSSION

Electronic properties of $Ga_xSi_{1-x}C$ NT

In this section, we present the calculated majority- and minority-spin band structures, total density of states (TDOS), and partial density of states (PDOS) for Ga-doped SWSiCNTs, in which Ga atoms substitute for Si sites. In addition to the electronic structure analysis, Bader charge calculations were performed to examine charge redistribution induced by Ga doping. The focus is placed on two doping concentrations 8.3% (single substitution) and 16.6% (double substitution) to investigate how varying dopant levels influence the electronic and magnetic properties of SiCNTs. Understanding these effects is critical for tailoring SiCNTs toward nanoelectronic and spintronic applications. From first-principles calculations, spin-resolved band gaps were obtained and are illustrated in Figs. 1 and 2. Figure 1shows the spin-dependent band structures of Ga-doped SWSiCNTs, confirming semiconducting behavior in both spin-up and spin-down channels at low doping. Specifically, for the single Ga-doped system (8.3% concentration), where one Si atom is replaced by Ga, the estimated band gaps are ~1.0 eV for the majority-spin states and ~0.6 eV (direct) and ~0.5 eV (indirect) for the minority-spin states.

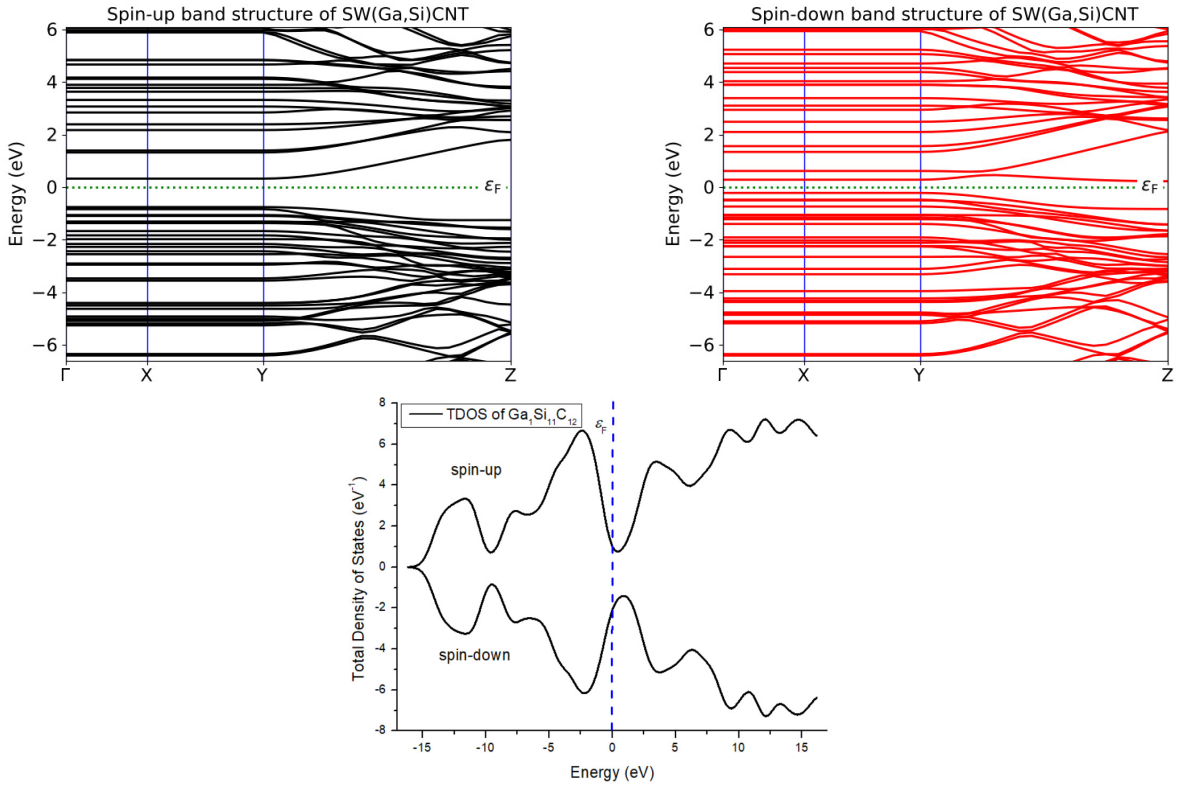

Figure 1. Spin-polarized band structures (spin-up: black, spin-down: red) and the corresponding total density of states (TDOS) for the studied $Ga_xSi_{1-x}C$ NTs

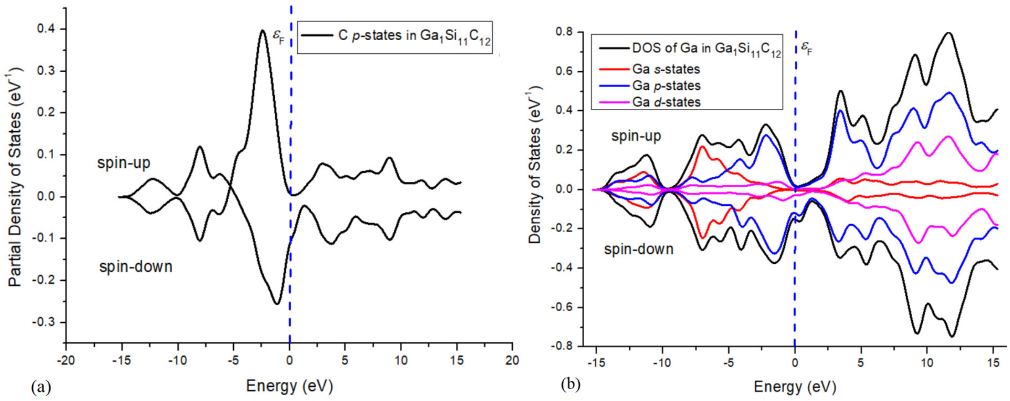

Figure 2. PDOS of C (a) and Ga (b) atoms in $Ga_xSi_{1-x}C$ nanotubes, with positive/negative values denoting majority/minority spin states

In contrast, for the double Ga-doped configuration (16.6% concentration), where two Si atoms are substituted by Ga, the spin-up channel retains a semiconducting gap of ~1.2 eV. However, in the spin-down channel, the bands cross the Fermi level, producing a vanishing band gap. This pronounced spin asymmetry reveals a half-metallic character, a key property for spintronic device applications.

First-principles simulations show that Ga doping significantly modifies the electronic structure of the (6,0) SWSiCNT. In the single-doped system, the minority-spin band gap is reduced to 0.5 eV, while the majority-spin channel remains semiconducting. Partial density of states (PDOS) analysis reveals that states near the Fermi level are predominantly derived from the C 2p and Ga 5d orbitals. In particular, the notable contribution of Ga 5d orbitals at the Fermi energy highlights a moderate orbital interaction between Ga and neighboring C atoms.

Table 1 summarizes the calculated spin-resolved band gaps for Ga-doped SWSiCNTs at different doping levels. The pristine nanotube exhibits a semiconducting band gap of 0.98 eV, consistent with our earlier findings [21]. At 8.3% Ga doping (single substitution at a Si site), the system displays spin asymmetry, with a 1.0 eV gap in the spin-up channel and reduced gaps of 0.6 eV (direct) and 0.5 eV (indirect) in the spin-down channel. This confirms the preservation of semiconducting behavior, albeit with distinct spin-dependent gaps.

In contrast, at 16.6% Ga doping (double substitution), the spin-up channel retains a semiconducting gap of ~1.2 eV, while the spin-down bands cross the Fermi level, closing the gap entirely. This spin asymmetry establishes a robust half-metallic state, underscoring the potential of Ga-doped SWSiCNTs as promising candidates for spintronic devices, where spin-selective conductivity is essential.

Table 1. Spin-resolved band gaps (↑ , ↓) of Ga-doped SWSiCNTs at varying doping levels

System	Doping level	Band gap (eV)	Electronic Nature	Remarks
SWSiCNT (undoped)	0%	0.98	Semiconductor	Previous work [21]
SWSiCNT (Ga at Si site)	8.3%	1.0 (↑), 0.6 (direct) (↓), 0.5 (indirect) (↓)	Semiconductor	Spin asymmetry; majority spin semiconducting, minority spin nearly metallic
SWSiCNT (2 Ga at Si sites)	16.6%	1.2 (↑), 0 (↓)	Half-metal	Spin-down bands cross Fermi level

To further investigate the electronic interactions in Ga-doped SWSiCNTs, where Ga substitutes a Si atom, Bader charge analysis was carried out. The results reveal a distinct redistribution of charge upon doping. The Ga dopant exhibits a net Bader charge of approximately −1.05 e, notably less negative than the substituted Si atom (−2.33 e). This indicates that Ga contributes fewer electrons to the lattice, a consequence of its lower electronegativity and larger atomic radius compared to Si. The neighboring carbon atoms, particularly C14 the atom closest to the Ga site acquire a charge of about +1.94 e, which is lower than the typical ~+2.3 e gain observed for C atoms adjacent to Si. This reduction points to a weaker covalent character in the Ga-C interaction relative to the original Si-C bond, potentially altering the local electronic and magnetic properties.

In summary, Bader charge analysis confirms that Ga substitution at the Si site reduces charge transfer to the surrounding lattice. This diminished electron donation, along with weaker orbital hybridization with neighboring C atoms, aligns with the reduced spin polarization observed in the electronic structure.

Magnetic properties of $Ga_xSi_{1-x}C$ NT

We investigated the magnetic properties of Ga-doped (6,0) SiCNTs, focusing on substitutional doping at the Si site. To assess the magnetic behavior, we computed the atomic and total magnetic moments and compared ferromagnetic (FM) and antiferromagnetic (AFM) configurations to identify the most stable magnetic phase. Additionally, electron difference density plots were analyzed to visualize charge redistribution induced by Ga doping, highlighting the interaction between the Ga dopant and neighboring Si and C atoms. This combined analysis of spin-polarized electronic structure, magnetic moments, and local charge transfer provides a comprehensive view of the magnetic response introduced by Ga substitution.

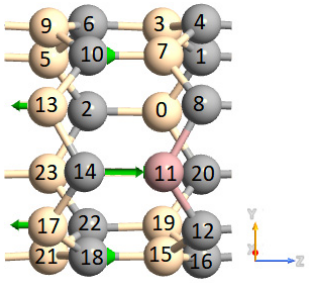

Figure 3. Spin-polarized structure of $Ga_xSi_{1-x}C$ nanotubes, with Si (beige), C (grey), Ga (pink), and magnetic moments (green arrows)

The Mulliken spin analysis shows that a single Ga substitution yields a total magnetic moment of ~1.0 μ_B, confirming the emergence of spin polarization (Fig. 3). Interestingly, the Ga atom itself carries a negative spin magnetic moment of −0.336 μ_B, acting as a localized magnetic impurity. The strongest positive spin polarization is observed on adjacent carbon atoms, with C14 exhibiting a significant magnetic moment of ~1.6 μ_B. Additional contributions come from C10 and C18, each exceeding 0.4 μ_B. In contrast, nearby Si atoms, such as Si13 and Si17, show negative spin moments of ~−0.5 μ_B, indicating antiparallel coupling with the polarized carbon atoms. This distribution suggests that magnetism in the single-doped system originates mainly from induced spin polarization on carbon atoms, partially compensated by negative contributions from Ga and its neighboring Si atoms.

When two Ga atoms are introduced, the total spin magnetic moment nearly doubles to ~2.0 μ_B, suggesting largely additive contributions from each dopant. The Ga atoms exhibit stronger negative spin moments (~−0.57 μ_B), reinforcing their role as localized magnetic impurities. Several neighboring carbon atoms, including C1, C4, C8, C12, and C20, display enhanced positive magnetic moments close to or exceeding 1.0 μ_B, revealing stronger spin polarization in the carbon sublattice compared to the single-doped case. Although silicon atoms continue to exhibit negative spin moments, their magnitudes are somewhat reduced, likely due to overlapping spin polarization fields from multiple dopants.

Overall, the magnetism in Ga-doped SiCNTs arises from a complex interplay between localized negative spin moments on Ga and Si atoms and strong positive polarization on specific carbon atoms. In the double-doped system, the overlapping polarization fields enhance the net magnetization while simultaneously modulating local spin distributions. These findings highlight the critical role of carbon atoms as hosts of induced magnetic moments, while silicon atoms mediate spin coupling in the doped nanotube.

The orbital analysis reveals a pronounced redistribution of electronic charge and spin polarization around the Ga dopant and its neighboring atoms. For the three carbon atoms directly bonded to Ga, strong occupation of the p-orbitals, particularly the p_x and p_y components, correlates with the substantial positive spin magnetic moments observed in these sites. In contrast, the Ga dopant itself exhibits dominant s and p-orbital occupation, but with relatively small spins contributions. This behavior reflects Ga's role as an electron acceptor and a weakly magnetic center rather than a strong contributor to the net magnetization. Surrounding silicon atoms display negative spin polarization, arising mainly from their p-orbitals. These negative contributions compensate for the spin accumulation localized on nearby carbon atoms, thereby influencing the overall balance of magnetic interactions within the nanotube.

Table 2 summarizes the calculated spin magnetic moments (in μ_B) for individual atoms in SiCNTs with one and two Ga dopants substituting Si sites. The results demonstrate how Ga incorporation systematically modifies local spin distributions, clarifying the mechanisms by which Ga affects the overall magnetic properties of the SiCNT system.

Table 2. Magnetic moments (μ_B) of atoms in Ga-doped (6,0) SiCNTs at Si sites

No.	Element	Spin Moment (1 Ga-doped)	Spin Moment (2 Ga-doped)
0	Si	-0.002	-0.574 (Ga)
1	C	-0.001	1.036
2	C	0.010	0.474
3	Si	-0.028	-0.582
4	C	0.095	0.891
5	Si	-0.006	-0.376
6	C	0.011	0.153
7	Si	-0.167	-0.582
8	C	0.183	1.036
9	Si	-0.137	-0.253
10	C	0.408	0.154
11	Ga	-0.336	-0.573
12	C	0.183	1.035
13	Si	-0.500	-0.375
14	C	1.612	0.470
15	Si	-0.167	-0.582
16	C	0.095	0.892
17	Si	-0.500	-0.375
18	C	0.408	0.154
19	Si	-0.028	-0.582
20	C	-0.001	1.036
21	Si	-0.137	-0.253
22	C	0.011	0.154
23	Si	-0.006	-0.376
	Sum	**1.001**	**2.002**

The results clearly establish that carbon atoms play a central role in sustaining and amplifying the magnetization induced by Ga doping, with certain carbon sites exhibiting particularly large spin magnetic moments. In contrast, the negative spin moments on Ga and nearby Si atoms reflect antiferromagnetic coupling, which partially offsets the positive contributions from carbon. As a result, the net magnetic moment is smaller than the simple sum of absolute spin values. Importantly, the nearly linear increase in total magnetization when moving from one to two Ga dopants indicates that magnetic contributions from individual Ga atoms and their surrounding carbon environments add constructively, with minimal magnetic quenching. Such behavior highlights the tunability of magnetism in SiCNTs through controlled doping strategies, which is highly relevant for spintronic applications requiring specific spin configurations. These findings also emphasize the importance of both dopant concentration and the local atomic environment in tailoring magnetic behavior within low-dimensional semiconductor nanostructures.

Figure 4 depicts the charge density redistribution caused by substitutional Ga doping at a Si site. The purple regions represent electron accumulation, primarily localized around the Ga dopant and adjacent carbon atoms, while the

cyan regions indicate electron depletion, largely concentrated near the replaced Si site. This charge transfer pattern underscores the modified bonding interactions between Ga and the host nanotube lattice, offering critical insight into how Ga incorporation alters the local electronic environment and, consequently, the overall electronic properties of the system.

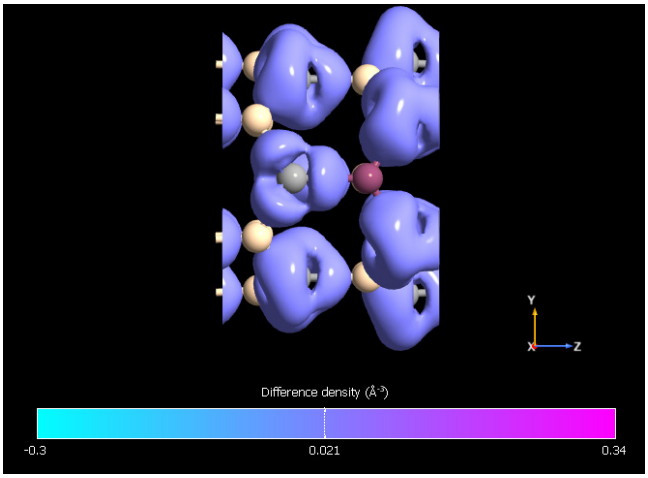

Figure 4. Spin density isosurface of Ga-doped SWSiCNT at the Si site, showing charge accumulation (purple) and depletion (cyan). Si, C, and Ga atoms are represented by beige, gray, and pink spheres, respectively

The total energy comparison between ferromagnetic (FM) and antiferromagnetic (AFM) states reveals that the AFM configuration is energetically more favorable. Specifically, the calculated total energies are −4108.82776 eV for the FM state and −4108.92690 eV for the AFM state, yielding a positive energy difference in favor of AFM ordering. This result indicates that Ga-doped (6,0) SWSiCNTs prefer an antiferromagnetic ground state. The emergence of such magnetic ordering highlights their potential as nanoscale magnetic materials, making them promising candidates for spintronic and nanomagnetic device applications.

Formation energies of Ga-doped (6,0) SWSiCNTs

Defect formation and dopant incorporation are critical factors in shaping the physical and chemical properties of nanoscale materials. The formation energy of a defect structure quantifies the energetic cost of introducing dopants into the host lattice and serves as a key indicator of thermodynamic stability. A lower formation energy implies a more stable and experimentally accessible configuration, facilitating dopant incorporation during material synthesis and device fabrication. In contrast, high formation energies suggest that a given doped structure may be challenging to achieve or maintain, limiting its practical applicability.

In this study, the formation energies of both single and double Ga-doped (6,0) SWSiCNTs were calculated at substitutional Si sites to assess their stability and likelihood of experimental realization. These values provide essential insight into the feasibility of controlled Ga doping for tailoring the electronic and magnetic properties of SiCNTs in future spintronic and nanoelectronic applications.

The formation energy $E_{\text{form.}}$ was calculated using the following expression:

$$E_{form.} = E_{doped} - E_{pristine} - n \cdot \mu_{Ga} + n \cdot \mu_{Si} \tag{5}$$

where E_{doped} and E_{pristine} are the total energies of the doped and pristine nanotubes, respectively; μ_{Ga} and μ_{Si} denote the chemical potentials of the dopant and substituted atoms; and n represents the number of dopants (1 for single doping and 2 for double doping).

In this study, the chemical potential values of Ga, Si, and C were taken as −2.228112 eV, −3.686924 eV, and −5.114380 eV, respectively. The total energy of the pristine nanotube, obtained from our calculations, was E_{pristine}=−3983.35741 eV. These values were used to determine the defect formation energies for all doping configurations.

Table 3 presents the calculated formation energies for single and double Ga doping at Si substitutional sites, providing a comparative overview of the thermodynamic stability across different configurations.

Table 3. Total (E_{doped}) and formation ($E_{\text{form.}}$) energies of single- and double-Ga-doped SiCNTs at Si sites, with dopant concentration x (%) indicated

System	x, %	E_{doped}, eV	E_{form}, eV
$Si_{11}Ga_1C_{12}$	8.3	-4046.11780	-64.21920
$Si_{10}Ga_2C_{12}$	16.6	-4108.82776	-128.3887

The results show that Ga doping at Si sites consistently yields negative formation energies, confirming that Ga incorporation is energetically favorable and stabilizes defect structures within SiC nanotubes. Moreover, the

increasingly negative values observed for double doping indicate that higher Ga concentrations are thermodynamically preferred. This trend suggests that Ga not only integrates stably into the nanotube lattice but also enhances structural stability as the doping level increases. The total energy decreases with increasing Ga concentration, indicating enhanced stabilization of the doped nanotube structure.

Figure 4 represents the variation of total energy (E_{doped}) and formation energy ($E_{form.}$) of Ga-doped SiCNTs with dopant concentration (x). The decreasing trend of both energies with increasing Ga content indicates that Ga substitution at Si sites enhances the structural stability and thermodynamic favorability of the nanotubes.

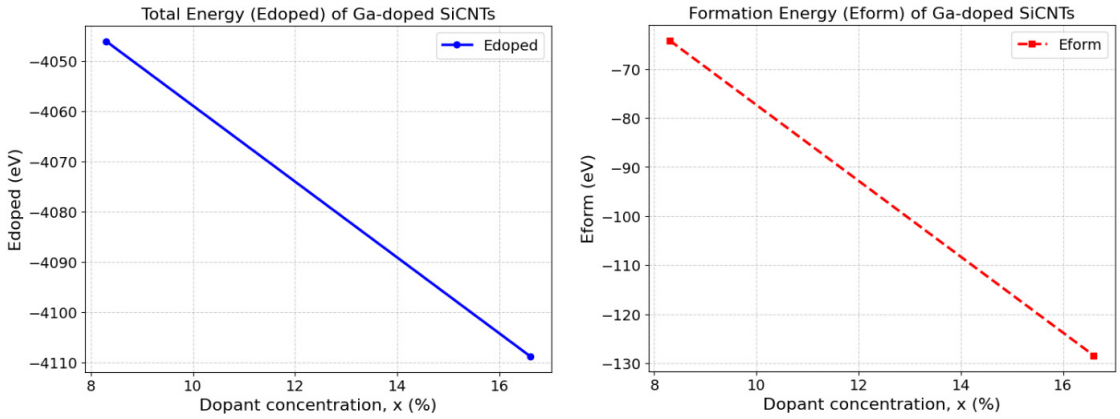

Figure 5. Variation of total (E_{doped}) and defect-formation energies ($E_{form.}$) of Ga-doped SWSiCNTs with dopant concentration (x=8.3 and 16.6 %)

These results suggest that Ga substitution enhances the thermodynamic stability of SWSiCNTs, making them more favorable at higher dopant concentrations. The decreasing energies further suggest that Ga doping may induce beneficial modifications to the nanotubes' electronic and structural properties, which could benefit applications in nanoelectronics and sensing devices.

These findings complement the magnetic ground state analysis, providing a comprehensive understanding of both the energetic favorability and practical feasibility of Ga doping in SWSiCNTs. The preference for Si substitutional sites aligns with Ga's known chemical and electronic compatibility with semiconductor lattices, reinforcing its suitability as a dopant. Collectively, the results highlight Ga's effectiveness in stabilizing the SiCNT framework, guiding future experimental efforts to optimize doped nanotubes for spintronic and nanoelectronic devices.

4. CONCLUSIONS

In this study, first-principles calculations were employed to systematically investigate the influence of Ga doping on the electronic and magnetic properties of (6,0) single-walled silicon carbide nanotubes (SWSiCNTs). The results demonstrate that Ga substitution at Si sites induces pronounced spin asymmetry and drives the system toward a half-metallic state at higher doping concentrations, thereby enhancing its potential for spintronic applications.

Bader charge and orbital analyses reveal that Ga substitution reduces charge transfer relative to pristine SiCNTs, weakening covalent bonding and modifying the local electronic environment. The induced magnetism originates primarily from neighboring carbon atoms, which develop strong positive spin polarization, while Ga and nearby Si atoms exhibit negative spin moments that couple antiferromagnetically. The total magnetic moment increases nearly linearly with doping concentration, and energy calculations confirm that the AFM state is the preferred ground state.

The negative formation energies of both single and double Ga doping configurations confirm the thermodynamic stability and experimental feasibility of Ga incorporation at Si sites. These results highlight Ga-doped SiCNTs as a robust and versatile material platform for engineering nanoscale magnetism and electronic behavior. Overall, this work offers valuable theoretical insights to guide the design and optimization of doped SiCNTs for advanced applications in spintronics and nanoelectronics.

ORCID

V.N. Jafarova, https://orcid.org/0000-0002-0643-1464; **Kh.A. Hasanova**, https://orcid.org/0009-0002-0476-0077
A.A. Guliyeva, https://orcid.org/0009-0004-7405-3049; **V.I. Eminova,** https://orcid.org/0009-0003-6827-9191
I.C. Scurtu, https://orcid.org/0000-0003-3105-6384

REFERENCES

[1] E.C. Ahn, "2D materials for spintronic devices," npj 2D Materials and Applications, **4**, 17 (2020). https://doi.org/10.1038/s41699-020-0152-0
[2] Md. M. Uddin, *et al*., "Graphene-like emerging 2D materials: recent progress, challenges and future outlook," RSC Advances, **13**, 33336–33375 (2023). https://doi.org/10.1039/D3RA04456D
[3] Md. A. Islam, *et al*., "Recent advances of 2D materials in semiconductor application: A review," Advanced Sensor and Energy Materials, **100161** (2025). https://doi.org/10.1016/j.asems.2025.100161

[4] B. Baumeier, P. Krüger, and J. Pollmann, "Structural, elastic, and electronic properties of SiC, BN, and BeO nanotubes," Physical Review B, **76**, 085407 (2007). https://doi.org/10.1103/PhysRevB.76.085407
[5] C.L. Frewin, C. Locke, S.E. Saddow, and E.J. Weeber, "Single-crystal cubic silicon carbide: an in vivo biocompatible semiconductor for brain–machine interface devices," Proceedings of the Annual International Conference of the IEEE Engineering in Medicine and Biology Society, 2957–2960 (2011). https://doi.org/10.1109/IEMBS.2011.6090582
[6] J.S. Ponraj, S.C. Dhanabalan, G. Attolini, and G. Salviati, "SiC nanostructures toward biomedical applications and its future challenges," Critical Reviews in Solid State and Materials Sciences, **41**, 430–446 (2016). https://doi.org/10.1080/10408436.2016.1150806
[7] S.E. Saddow, C. Frewin, *et al.,* "Single-crystalline silicon carbide: A biocompatible and hemocompatible semiconductor for advanced biomedical applications," Materials Science Forum, **679–680**, 824–830 (2011). https://doi.org/10.4028/www.scientific.net/MSF.679-680.824
[8] S.M.S.H. Rafin, *et al*.: "Power electronics revolutionized: A comprehensive analysis of emerging wide and ultrawide bandgap devices," Micromachines, **14**(11), 2045 (2023). https://doi.org/10.3390/mi14112045
[9] M.A. Mahdy, S.H. Kenawy, E.M.A. Hamzawy, G.T. El-Bassyouni, and I.K. El Zawawi, "Influence of silicon carbide on structural, optical and magnetic properties of Wollastonite/Fe_2O_3 nanocomposites," Ceramics International, **47**(9), 12047–12055 (2021). https://doi.org/10.1016/j.ceramint.2021.01.048
[10] A. Du, and S.C. Smith, "Silicon carbide nanotubes functionalized by transition metal atoms: a density functional study," The Journal of Physical Chemistry C, **111**(52), 20295–20300 (2007). https://doi.org/10.1021/jp073722m
[11] S. Yan, *et al*., "Transition metal induced magnetization in zigzag silicon carbide nanotubes," Journal of Computational Electronics, **22**, 203–212 (2023). https://doi.org/10.1007/s10825-023-02030-y
[12] J.X. Zhao, and Y.H. Ding, "Silicon carbide nanotubes functionalized by transition metal atoms: A density-functional study," The Journal of Physical Chemistry C, **112**, 2558–2564 (2008). https://doi.org/10.1021/jp073722m
[13] H. Heidarzadeh, "Transition metal-doped 3C-SiC as a promising material for intermediate band solar cells," Optical and Quantum Electronics, **51**, 32 (2019). https://doi.org/10.1007/s11082-019-1742-y
[14] A.T. Mulatu, K.N. Nigussa, and L.D. Deja, "Electronic and optical properties of TM-doped (8,0) SiC single-walled nanotubes and the prospect of hydrogen storage," *Optical Materials*, **134**, 113094 (2022). https://doi.org/10.1016/j.optmat.2022.113094
[15] Ch. Vatankhah, and H.A. Badehian, "Electronic and optical properties of armchair silicon carbide nanotubes from first principles," Optik, **237**, 166740 (2021). https://doi.org/10.1016/j.ijleo.2021.166740
[16] W. Wang, J. Xu, Y. Zhang, and G. Li, "First-principles study of electronic structure and optical properties of silicon/carbon nanotube," Computational Chemistry, **5**, 159–171 (2017). https://doi.org/10.4236/cc.2017.54013
[17] M.N. Huda, and A. Ray, "Evolution of SiC nanocluster from carbon fullerene: A density functional theoretic study," Chemical Physics Letters, **457**(1–3), 124–129 (2008). https://doi.org/10.1016/j.cplett.2008.03.057
[18] R.Z. Ibaeva, V.N. Jafarova, V.I. Eminova, I.C. Scurtu, and S. Lupu, "First-principles study of electronic and magnetic properties of Ag- and Au-doped single-walled (6,0) SiC nanotubes: DFT study," Journal of Nanoparticle Research, **26**(9), 203 (2024). https://doi.org/10.1007/s11051-024-06109-w
[19] V.N. Jafarova, S.S. Rzayeva, I.C. Scurtu, C. Stanca, N. Acomi, and G. Raicu, "Prediction of ferromagnetism in GaN:Ag and SiC:Ag nanotubes," Advances in Natural Sciences: Nanoscience and Nanotechnology, **15**(3), 035012 (2024). https://doi.org/10.1088/2043-6262/ad71a7
[20] V.N. Jafarova, V.I. Eminova, M.A. Musaev, and I.C. Scurtu, "Prediction of ferromagnetic characteristics of gold-doped SiC nanotubes for application in spintronic devices," Technium, **26**, 1–8 (2025). https://doi.org/10.47577/technium.v26i.12149
[21] N.T. Tien, P.T.B. Thao, V.N. Jafarova, and D. Dey Roy, "Predicting model for device density of states of quantum-confined SiC nanotube with magnetic dopant: An integrated approach utilizing machine learning and density functional theory," Silicon, 1–19 (2024). https://doi.org/10.1007/s12633-024-03127-0
[22] S. Rzayeva, V.N. Jafarova, and D.D. Roy, "First-principles prediction of ferromagnetism and Curie temperature for transition metals doped single-walled (6,0) SiC nanotubes: Materials for application in spintronics," Materials Science in Semiconductor Processing, **197**, 109702 (2025). https://doi.org/10.1016/j.mssp.2025.109702
[23] S. Rzayeva, and V.N. Jafarova, "Electronic and magnetic properties of cobalt-doped SiCNT: A first-principles study," Journal of Polytechnic, **28**(3), 947–955 (2025). https://doi.org/10.2339/politeknik.1536597
[24] A.Q. Wu, Q.G. Song, and L. Yang, "First-principles study on Al or/and P doped SiC nanotubes," Advanced Materials Research, **510**, 747–752 (2012). https://doi.org/10.4028/www.scientific.net/AMR.510.747
[25] A.A. Peyghan, A. Soltani, A.A. Pahlevani, Y. Kanani, and S. Khajeh, "A first-principles study of the adsorption behavior of CO on Al- and Ga-doped single-walled BN nanotubes," Applied Surface Science, **270**, 25–32 (2013). https://doi.org/10.1016/j.apsusc.2012.12.008
[26] M.D. Mohammadi, H.Y. Abdullah, G. Biskos, and S. Bhowmick, "Effect of Al- and Ga-doping on the adsorption of H_2SiCl_2 onto the outer surface of boron nitride nanotube: A DFT study," Comptes Rendus Chimie, **24**(2), 291–304 (2021). https://doi.org/10.5802/crchim.87
[27] H. Tavakol, and H. Haghshenas, "A DFT study on the interaction of doped carbon nanotubes with H_2S, SO_2, and thiophene," Quantum Reports, **3**(3), 366–375 (2021). https://doi.org/10.3390/molecules26030223
[28] S.S. Hardisty, X. Lin, A.R.J. Kucernak, and D. Zitoun, "Single-atom Pt on carbon nanotubes for selective electrocatalysis," Carbon Energy, **6**(1), e409 (2023). https://doi.org/10.1002/cey2.409
[29] Y.S. Itas, R. Razali, S. Tata, A.M. Idris, and M.U. Khandaker, "Studies of the hydrogen energy storage potentials of Fe- and Al-doped silicon carbide nanotubes (SiCNTs) by optical adsorption spectra analysis," Journal of Energy Storage, **72**, 108534 (2023). https://doi.org/10.1016/j.est.2023.108534
[30] W. Liu, Q. Li, X. Yang, X. Chen, and X. Xu, "Synthesis and characterization of N-doped SiC powder with enhanced photocatalytic and photoelectrochemical performance," Catalysts, **10**, 769 (2020). https://doi.org/10.3390/catal10070769

[31] U. Adharsh, R. Akash, A. Sakthi Balaji, D. John Thiruvadigal, R.M. Hariharan, J. Sneha, V. Abinaya, and K.J. Sivasankar, "Chemical functionalization of silicon carbide nanotube (SiCNT): First principles DFT study," ECS Journal of Solid State Science and Technology, **12**, 111001 (2023). https://doi.org/10.1149/2162-8777/ad0327
[32] S.I. Vlaskina, *et al*., "Nano silicon carbide's stacking faults, deep levels and grain boundary defects," Journal of Nano- and Electronic Physics, **10**(5), 05021 (2018). https://doi.org/10.21272/jnep.10(5).05021
[33] W. Kohn, and L.J. Sham, "Self-consistent equations including exchange and correlation effects," Physical Review, **140**, A1133–A1138 (1965). https://doi.org/10.1103/PhysRev.140.A1133
[34] V.N. Jafarova, "Structural, electronic and magnetic properties of pure and Fe-doped ZnSe: First-principles investigation," Pramana – Journal of Physics, **98**, 82–93 (2024). https://doi.org/10.1007/s12043-024-02752-z
[35] M. Fuchs, and M. Scheffler, "Ab initio pseudopotentials for electronic structure calculations of polyatomic systems using density functional theory," Computer Physics Communications, **119**, 67–98 (1999). https://doi.org/10.1016/S0010-4655(98)00201-X
[36] M. Cococcioni, and S. de Gironcoli, "A linear response approach to the calculation of the effective interaction parameters in the LDA+U method," *Physical Review B*, **71**, 035105 (2005). https://doi.org/10.1103/PhysRevB.71.035105
[37] S.L. Dudarev, G.A. Botton, S.Y. Savrasov, C.J. Humphreys, and A.P. Sutton, "Electron-energy-loss spectra and the structural stability of nickel oxide: An LSDA+U study," Physical Review B, **57**, 1505–1509 (1998). https://doi.org/10.1103/PhysRevB.57.1505
[38] A.I. Liechtenstein, V.I. Anisimov, and J. Zaanen, "Density-functional theory and strong interactions: Orbital ordering in Mott–Hubbard insulators," Physical Review B, **52**, R5467–R5470 (1995). https://doi.org/10.1103/PhysRevB.52.R5467
[39] S.C. North, K.R. Jorgensen, J. Pricetolstoy, and A.K. Wilson, "Population analysis and the effects of Gaussian basis set quality and quantum mechanical approach: Main group through heavy element species," Frontiers in Chemistry, **11**, 1152500 (2023). https://doi.org/10.3389/fchem.2023.1152500
[40] W. Gough, "The graphical analysis of a Lorentzian function and a differentiated Lorentzian function," Journal of Physics A: General Physics, **1**, 704–709 (1968). https://doi.org/10.1088/0305-4470/1/6/309
[41] H.J. Monkhorst, and J.D. Pack, "Special points for Brillouin-zone integrations," Physical Review B, **13**, 5188–5192 (1976). https://doi.org/10.1103/PhysRevB.13.5188

ПЕРШОПРИНЦИПНІ ДОСЛІДЖЕННЯ ЕЛЕКТРОННИХ ТА МАГНІТНИХ ВЛАСТИВОСТЕЙ НАНОТРУБОК КАРБІДУ КРЕМНІЮ, ЛЕГОВАНИХ ГАЛІЄМ

Вусала Набі Джафарова[1], Хаяла Аждар Гасанова[1,2], Аділя Адем Гулієва[3], Вусала Іршад Емінова[4], Іонут Крістіан Скурту[5]

[1]Азербайджанський державний університет нафти та промисловості, 20 пр. Азаліг, AZ-1010, Баку, Азербайджан
[2]Міністерство науки та освіти Азербайджанської Республіки, Інститут фізики, просп. Г. Джавіда, 131, AZ-1143, Баку, Азербайджан
[3]Державний університет Нахчівана, AZ 7012 Нахчіван, Азербайджан
[4]Франко-Азербайджанський університет (UFAZ) при Азербайджанському державному університеті нафти і промисловості Вулиця Нізамі, 183 AZ-1010, Баку Азербайджан
[5]Військово-морська академія Мірчі Старшого, вулиця Фулгерулуй, 1, 900218, Констанца, Румунія

Ця робота досліджує електронні та магнітні характеристики нанотрубок карбіду кремнію (SiCNT), легованих галієм (Ga), за допомогою першопринципних розрахунків. Розглянуто два рівні легування (8,3% і 16,6%), де атоми Ga заміщують атоми кремнію в одностінних (6,0) SiCNT. Аналіз спін-поляризованої зонної структури показує, що система змінюється від напівпровідникової при нижчому рівні легування до напівметалічної при вищих концентраціях, що свідчить про значний потенціал для застосувань у спінтроніці. Аналіз густини станів і зарядів за Бадером демонструє, що введення Ga змінює розподіл заряду та орбітальні взаємодії, зокрема між станами Ga 5d та C 2p. Розрахунки магнітного моменту показують, що Ga індукує локалізований магнетизм переважно на сусідніх атомах вуглецю, а загальна намагніченість зростає зі збільшенням рівня легування. Порівняння енергій для феромагнітної та антиферомагнітної конфігурацій вказує на антиферомагнітний основний стан, тоді як оцінка енергії утворення підтверджує термодинамічну сприятливість заміщення Ga у позиціях Si. Загалом отримані результати підкреслюють, що Ga-леговані SiCNT є перспективними та керовано налаштовуваними матеріалами для майбутніх наноелектронних і спінтронних пристроїв.

Ключові слова: *SiC:Ga, нанотрубка; магнітний момент; напівметалічний*